Development of pulmonary fibrosis through a pathway involving the transcription factor Fra-2/AP-1

Robert Eferl*†‡, Peter Hasselblatt*‡§, Martina Rath*, Helmut Popper¶, Rainer Zenz†, Vukoslav Komnenovic*, Maria-Helena Idarraga*, Lukas Kenner†‖, and Erwin F. Wagner*,**

*Research Institute of Molecular Pathology, Doktor Bohr-Gasse 7, A-1030 Vienna, Austria; †Ludwig Boltzmann Institute for Cancer Research, Währinger Strasse 13a, A-1090 Vienna, Austria; §Department of Medicine II, University of Freiburg, Hugstetter Strasse 55, D-79106 Freiburg, Germany; ¶Institute of Pathology, Medical University of Graz, Auenbruggerplatz 25, A-8036 Graz, Austria; and ‖Institute of Clinical Pathology, Medical University of Vienna, Währinger Gürtel 18-20, A-1090 Vienna, Austria

Edited by Michael Karin, University of California at San Diego School of Medicine, La Jolla, CA, and approved May 12, 2008 (received for review February 14, 2008)

Studies using genetically modified mice have revealed fundamental functions of the transcription factor Fos/AP-1 in bone biology, inflammation, and cancer. However, the biological role of the Fos-related protein Fra-2 is not well defined *in vivo*. Here we report an unexpected profibrogenic function of Fra-2 in transgenic mice, in which ectopic expression of Fra-2 in various organs resulted in generalized fibrosis with predominant manifestation in the lung. The pulmonary phenotype was characterized by vascular remodeling and obliteration of pulmonary arteries, which coincided with expression of osteopontin, an AP-1 target gene involved in vascular remodeling and fibrogenesis. These alterations were followed by inflammation; release of profibrogenic factors, such as IL-4, insulin-like growth factor 1, and CXCL5; progressive fibrosis; and premature mortality. Genetic experiments and bone marrow reconstitutions suggested that fibrosis developed independently of B and T cells and was not mediated by autoimmunity despite the marked inflammation observed in transgenic lungs. Importantly, strong expression of Fra-2 was also observed in human samples of idiopathic and autoimmune-mediated pulmonary fibrosis. These findings indicate that Fra-2 expression is sufficient to cause pulmonary fibrosis in mice, possibly by linking vascular remodeling and fibrogenesis, and suggest that Fra-2 has to be considered a contributing pathogenic factor of pulmonary fibrosis in humans.

fra-2 transgenic mouse | idiopathic pulmonary fibrosis | osteopontin | pulmonary arterial hypertension | fibrosis mouse model

The transcription factor AP-1 is composed of Jun (c-Jun, JunB, JunD) and Fos proteins (c-Fos, FosB, Fra-1, Fra-2) which control a variety of stress responses, including cell proliferation, apoptosis, inflammation, wound healing, and cancer (1). Individual Fos proteins have been thoroughly studied in gain- and loss-of-function mouse models, which revealed important functions in bone cell proliferation and differentiation (2–4). Fra-2 is the least-studied Fos protein. It was recently demonstrated that loss of Fra-2 causes perinatal lethality (5), but there is no direct genetic evidence that Fra-2 or other Fos proteins are involved in the pathogenesis of fibroproliferative diseases.

Pulmonary fibrosis is a common and usually fatal end-stage condition of various lung diseases characterized by interstitial pneumonia and scarring. Inflammation is an important contributor in some subtypes of pulmonary fibrosis that have been associated with autoimmune diseases such as systemic sclerosis. However, the etiology is unknown in most cases, which are therefore classified as idiopathic pulmonary fibrosis (IPF) or nonspecific interstitial pneumonia (NSIP) (6). Although IPF was initially considered an autoimmune disease, there is no obvious correlation between the severity of inflammation and disease prognosis, and patients are largely unresponsive to immunosuppressive therapy (7). More recent data have proposed that IPF is an epithelial/mesenchymal disease resulting from repeated epithelial cell injury and aberrant wound healing (8, 9). Besides aberrant matrix production by mesenchymal cells, vascular remodeling of pulmonary arteries and pulmonary arterial hypertension have been identified as potential prognostic factors in IPF (10), but the relevance of these findings for the pathogenesis remains unclear (11, 12).

In this study, we report a profibrogenic activity of the Fos-related protein Fra-2. Ectopic expression of Fra-2 in transgenic mice caused fibrosis in several organs but mainly affected pulmonary tissues. Several growth factors, chemokines, and cytokines implicated in human pulmonary fibrosis were strongly expressed in diseased lungs of transgenic mice. Moreover, human samples of pulmonary fibrosis with IPF and NSIP showed strong immunoreactivity for Fra-2, suggesting that the pathomechanisms leading to pulmonary fibrosis in this transgenic mouse model may also be relevant for human disease.

Results

Fra-2 Transgenic (*fra-2*[tg]) Mice Develop Pulmonary Fibrosis. We have previously generated H2Kb-*c-fos* and H2Kb-*fra-1* transgenic mice to investigate the functions of these proteins in bone biology (2, 3). The same transgenic vector design was used here to generate *fra-2*[tg] mice in which the murine *fra-2* gene was expressed under control of the ubiquitous major histocompatibility complex class I antigen H2Kb promoter (Fig. 1*a*). An IRES-EGFP reporter gene was placed downstream of the genomic *fra-2* sequence to detect transgene expression. The 3′ long terminal repeat sequence of the Finkel–Biskis–Jinkins-murine sarcoma virus was linked to the 3′ end of the IRES-EGFP sequence to stabilize *fra*-2 mRNA and to ensure *fra*-2 expression in mesenchymal cells. Three transgenic founder lines (12, 13, and 15) were established for further analyses. Southern blot and quantitative PCR analyses demonstrated that founders 12, 13, and 15 harbored approximately 4, 60, and 3 transgene copies, respectively (Fig. 1*b* and data not shown). RNase-protection assays revealed transgene expression in various tissues of lines 12 and 13 [supporting information (SI) Fig. S1 and data not shown]. In contrast, no transgene expression was detectable in tissues of line 15 (data not shown). Transgenic mice of all lines were fertile, born in Mendelian ratio, and did not display any apparent early developmental abnormalities. Sur-

MEDICAL SCIENCES

Author contributions: R.E., P.H., and E.F.W. designed research; R.E., P.H., M.R., V.K., and M.-H.I. performed research; R.E., P.H., H.P., R.Z., L.K., and E.F.W. analyzed data; and R.E., P.H., and E.F.W. wrote the paper.

The authors declare no conflict of interest.

This article is a PNAS Direct Submission.

‡R.E. and P.H. contributed equally to this work.

**To whom correspondence should be sent at the present address: Cancer Cell Biology Program, Spanish National Cancer Center, Melchor Fernandez Almagro 3, E-28029 Madrid, Spain. E-mail: ewagner@cnio.es.

This article contains supporting information online at www.pnas.org/cgi/content/full/0801414105/DCSupplemental.

© 2008 by The National Academy of Sciences of the USA

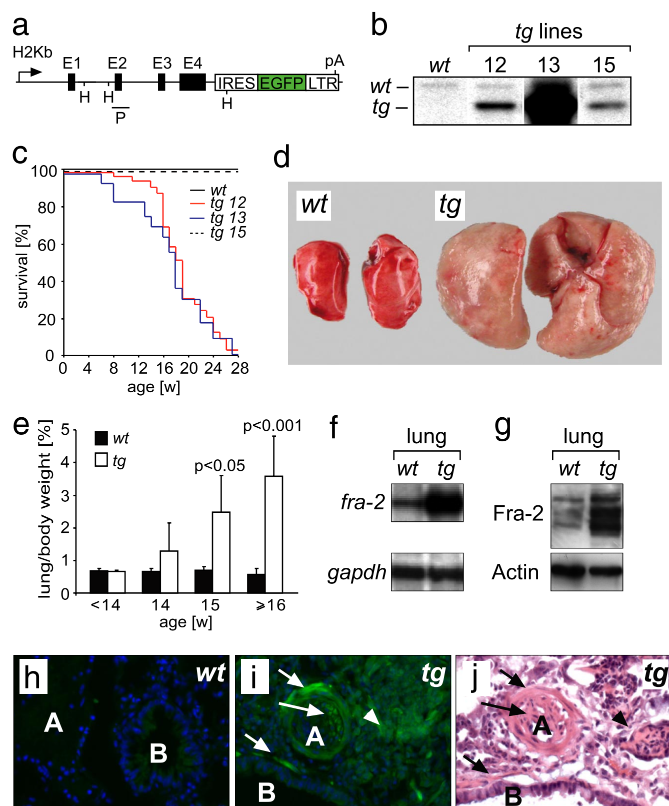

Fig. 1. Fra-2 gain-of-function approach. (*a*) Transgenic construct for ectopic expression of *fra-2 in vivo* consisting of an H2Kb promoter, the genomic *fra-2* locus, a reporter IRES-EGFP sequence, and a LTR sequence harboring a polyadenylation signal (pA). E1–E4 are Exons 1–4 of *fra-2*; HindIII (H) restriction sites and probe location (P) used for Southern blot analysis are indicated. (*b*) Southern blot analysis of tail DNA from wild-type mice (*wt*) and three independent *fra-2*^{tg} (*tg*) lines (12, 13, and 15) by using the probe shown in *a*. (*c*) Kaplan–Meier plot showing increased mortality of transgenic lines 12 and 13. Mortality was not increased in line 15, which did not express the transgene. (*d*) Lungs of *fra-2*^{tg} mice (*tg*, line 13, 20 weeks of age, $n > 20$) were increased in size. (e) Lung/body weight ratios of *fra-2*^{tg} (*tg*, line 13) mice were increased at 15 weeks of age ($n \geq 3$ mice per time point). (*f*) RNase-protection assay demonstrating *fra-2* transgene expression in lungs of adult *fra-2*^{tg} mice (line 13). *gapdh* was used as loading control. (*g*) Western blot analysis demonstrating ectopic expression of Fra-2 protein in the lungs of adult *fra-2*^{tg} mice (line 13). The protein band pattern is characteristic for Fra-2. Actin was used as loading control. (*h* and *i*) Direct fluorescence of lung sections demonstrating the cellular localization of transgene expression. (*h*) Only background signal was observed in *wt* controls. (*i*) Transgene-encoded EGFP-fluorescence was detectable in neointimal cells (long arrow), peribronchial cells and VSMCs (short arrows), and fibroblastic cells (arrowheads) of *fra-2*^{tg} mice (line 13, $n = 3$). Nuclei were counterstained with DAPI. (*j*) An adjacent section was stained with H&E to allow a better assessment of the structures indicated in *i*. A, artery; B, bronchus.

prisingly, transgenic mice of lines 12 and 13 died at a median age of 17 weeks with clinical signs of respiratory distress such as tachypnea and hunched posture (Fig. 1*c* and data not shown). Macroscopical examination of sick mice at this age revealed massively increased lung weight and pulmonary tissue stiffness (Fig. 1 *d* and *e*). Lung size was increased, which may be partly due to increased stiffness preventing collapse of pulmonary tissues after organ resection. Fibrosis with abundant collagen deposition was most apparent in the lung but appeared also in other organs such as skin, thymus, and the periportal tracts of the liver, stomach, esophagus, and heart, but not in the kidney (Fig. S1 and data not shown). Lines 12 and 13 also showed increased bone mass and rare tumor formation such as fibrosarcomas in the head/neck region (unpublished observations). Transgene RNA expression was readily detectable in the lungs of lines 12 and 13 (Fig. 1*f* and data not shown). Western blot analyses of protein extracts from lungs and other tissues demonstrated that the transgene gives rise to full-length Fra-2 protein (Fig. 1*g* and data not shown). Moreover, transgenic Fra-2 protein was fully functional because its expression rescued perinatal lethality of mice with targeted disruption of *fra-2* (data not shown). Transgene expression in diseased lungs was more precisely assessed by direct fluorescence of the transgene-encoded reporter EGFP. Weak EGFP fluorescence was present throughout the lung tissue but was most prominently observed in smooth muscle cells of pulmonary arteries and bronchi and neointimal cells as well as in fibroblastic proliferations (Fig. 1 *h*–*j*).

Histopathological Characterization of Pulmonary Fibrosis in *fra-2*^{tg} Mice. Proceeding fibrosis in *fra-2*^{tg} lungs was studied to identify early events of disease development (Fig. 2 *a*–*d*). No obvious defect in lung development and morphology was observed before 12 weeks of age. Apoptosis of alveolar epithelial cells has been proposed as an initial stimulus of pulmonary wound healing and fibrogenesis in mice (13). However, increased apoptosis as assessed by TUNEL staining and deregulated expression of apoptosis-related genes was not evident before the onset of fibrosis (Fig. S2 and data not shown). Obliteration of pulmonary arteries was the first apparent pathological alteration and frequently coincided with perivascular inflammation, whereas the bronchial architecture was not altered. Increased thickness of pulmonary artery walls was observed at 12 weeks of age and preceded the onset of fibrosis by 2–3 weeks (Fig. 2*f*). Vascular obliteration was characterized by massive formation of neointima induced by proliferation of vascular smooth muscle cells (VSMCs) as determined by immunohistochemical staining for the proliferation marker Ki67 and αSMA (Fig. 2 *g*–*i*). At later stages, more prominent interstitial inflammation, tissue damage, and deposition of collagen occurred (Fig. 2 *c* and *d*), and cellular structures resembling fibroblastic foci became apparent (magnification in Fig. 2*c*). The phenotype of end-stage, diseased *fra-2*^{tg} lungs resembled some aspects of human NSIP- and IPF-related usual interstitial pneumonia, including fibrosis, dense lymphocytic infiltration, hyperplasia of bronchus-associated lymphoid tissue, and the presence of honeycombing changes in the peripheral lung lobules (Fig. 2 *d* and *e*).

ECM Production and Inflammation in Pulmonary Fibrosis of *fra-2*^{tg} Mice. Production of ECM by activated fibroblasts called myofibroblasts is a hallmark of pulmonary fibrosis (14). ECM-producing myofibroblasts were also present in the diseased lungs of *fra-2*^{tg} mice (Fig. S3). Interestingly, most myofibroblasts expressed the epithelial marker cytokeratin 8/18 (Fig. S3). This finding suggests that the epithelial-to-mesenchymal transition is likely an important source of myofibroblasts in *fra-2*^{tg} lungs, which is consistent with previous findings in TGFβ-dependent pulmonary fibrosis (15). However, increased collagen production in ECM-producing cells was not mediated by Fra-2 in a cell-autonomous manner because deposition of collagen was not elevated in primary pulmonary fibroblasts of *fra-2*^{tg} mice *in vitro* and stimulation with the profibrogenic factors TGF-β_1 and IL-4 induced collagen production to a similar extent as in fibroblasts isolated from littermate controls (Fig. S3). These findings suggest that pulmonary fibrosis in *fra-2*^{tg} mice is not primarily induced by aberrant Fra-2-dependent ECM production of mesenchymal cells.

Inflammation is not a prominent feature of human IPF but is more pronounced in immune-mediated and idiopathic cases of NSIP. In diseased *fra-2*^{tg} lungs, mixed perivascular and peribronchial inflammatory infiltrates were present (Fig. S4). Reciprocal bone marrow reconstitution experiments were performed to

Fig. 2. Obliteration of pulmonary arteries precedes pulmonary fibrosis in *fra-2*^{tg} mice. (*a–d*) Time course analysis of pulmonary disease in *fra-2*^{tg} mice between weeks 12 and 17 identifying obliteration of pulmonary arteries as early event of pulmonary disease in transgenic mice (arrows in *b* and *c*; magnification in *b*; right magnification in *c*; $n > 5$ per time point). In contrast, pulmonary arteries in wild-type controls appeared normal (arrows in *a*). Arteriostenosis was followed by inflammation and the appearance of fibroblastic proliferations (arrowhead and left magnification in *c*). (*d* and *e*) The histological alterations at later stages resembled human NSIP- and IPF-related usual interstitial pneumonia. (Scale bars: 200 μm.) (*e*) A sample from a patient with IPF. The short arrow indicates an occluded vessel. (*f*) Quantification of arteriostenosis. Thickness of the vessel walls is given as a percentage of the vessel diameter ($n \geq 15$ vessels from at least three mice per time point). (*g* and *h*) Dual immunohistochemistry for α smooth muscle actin (αSMA) (red) and Ki67 (brown) at 14 weeks of age for wild-type (*g*) and *fra-2*^{tg} (*h*) mice. Arteriostenosis was caused by neointima formation due to proliferation of αSMA-expressing VSMCs (*h*, arrows). (*i*) Proliferation in the vascular wall was quantified by immunohistochemistry for Ki67. The amount of Ki67-positive nuclei is given in percentage ($n = 20$ vessels from two mice per genotype at 14 weeks of age).

investigate whether ectopic expression of *fra-2* in the bone marrow compartment contributes to development of pulmonary fibrosis. Importantly, no pulmonary fibrosis developed in wild-type mice that were reconstituted with *fra-2*^{tg} bone marrow. In contrast, pulmonary fibrosis developed in *fra-2*^{tg} animals that were reconstituted with wild-type bone marrow (Fig. 3 *a–c* and Table S1). The efficiency of reconstitution was evaluated by Southern blot (data not shown) and FACS analysis of transplanted bone marrow cells and splenocytes detecting transgene-encoded EGFP (Fig. S4). These data suggest that development of pulmonary fibrosis requires Fra-2 expression in pulmonary rather than inflammatory cells.

In a different approach, *fra-2*^{tg} mice lacking functional B and T lymphocytes were generated (*fra-2*^{tg}/*rag2*$^{-/-}$). The severity of pulmonary fibrosis was not altered in these mice (Fig. 3 *d–g*), indicating that T and B lymphocytes are not essential for the pathogenesis of pulmonary fibrosis.

Fig. 3. Transgenic Fra-2 expression in inflammatory cells is not required for pulmonary fibrosis in *fra-2*^{tg} mice. (*a–c*) Representative Chromotrop Anilin-blue (CAB) stainings of lungs after irradiation and bone marrow reconstitution using wild-type (*wt*) and *fra-2*^{tg} (*tg*) animals as recipients and donors. The wild-type control is shown in *a*. Wild-type recipients reconstituted with *fra-2*^{tg} bone marrow (BM) did not develop pulmonary fibrosis (*b*), whereas *fra-2*^{tg} animals reconstituted with wild-type bone marrow developed the disease (*c*). Collagen is stained in blue. (*d–g*) Breeding of *fra-2*^{tg} animals into a *rag2*-deficient genetic background (no functional B and T cells) did not ameliorate pulmonary fibrosis. Shown are CAB stainings demonstrating comparable collagen deposition (blue) in *fra-2*^{tg}/*rag2*$^{+/-}$ (*d*) and *fra-2*^{tg}/*rag2*$^{-/-}$ (*e*) mice ($n = 6$). Lung weight (*f*) ($n = 6$) and mortality (*g*) ($n \geq 10$) were equally increased in *fra-2*^{tg} and *fra-2*^{tg}/*rag2*$^{-/-}$ mice.

Molecular Factors Involved in Pulmonary Fibrosis of *fra-2*^{tg} Mice. Several growth factors, chemokines, and cytokines contribute to the pathogenesis of pulmonary fibrosis and are elevated in human patients (16). Among these profibrogenic factors is the AP-1 target gene osteopontin (17–20). In *fra-2*^{tg} lungs, osteopontin expression was significantly elevated at 12 weeks of age and increased thereafter (Fig. 4*a*). Osteopontin was predominantly expressed by alveolar macrophages and the alveolar epithelium (Fig. 4 *b* and *c*). These alterations were followed by strong expression of insulin-like growth factor 1 at 13 weeks of age (Fig. 4*d*). Interestingly, expression of TGFβ isoforms was not increased (Fig. S5), and phosphorylated Smad2, an indicator of TGFβ activity, could be detected only at late stages of disease (>17 weeks) by immunohistochemistry (data not shown). Among chemokines, strong expression of the proangiogenic chemokines CXCL5 and CXCL1, the mouse homolog of human CXCL8, was observed at 13 weeks of age (Fig. 4*d*). Expression of CCL19 was rather reduced in *fra-2*^{tg} lungs, whereas expression of CCL21 was unchanged, suggesting that these CCR7 ligands do not contribute to fibrosis in *fra-2*^{tg} mice. Among cytokines, elevated expression of IL-2, IL-4, IL-6, and GM-CSF (Fig. 4*e* and Fig. S5) was observed. At terminal stages of disease (20 weeks of age), additional expression of IL-1β, IFN-γ, CCL1, CCL2, CCL3, CCL4, CXCL2, CXCL10, and CXCL11 was observed (Fig. 4*f*). These data indicate that pulmonary fibrosis in *fra-2*^{tg} mice recapitulates the expression of several profibrogenic factors in human patients and suggest that osteopontin may be a key factor in disease pathogenesis (see proposed model in Fig. 4*g*).

Fra-2 Expression in Human Samples of Pulmonary Fibrosis. The human relevance of the data obtained in *fra-2*^{tg} transgenic mice was

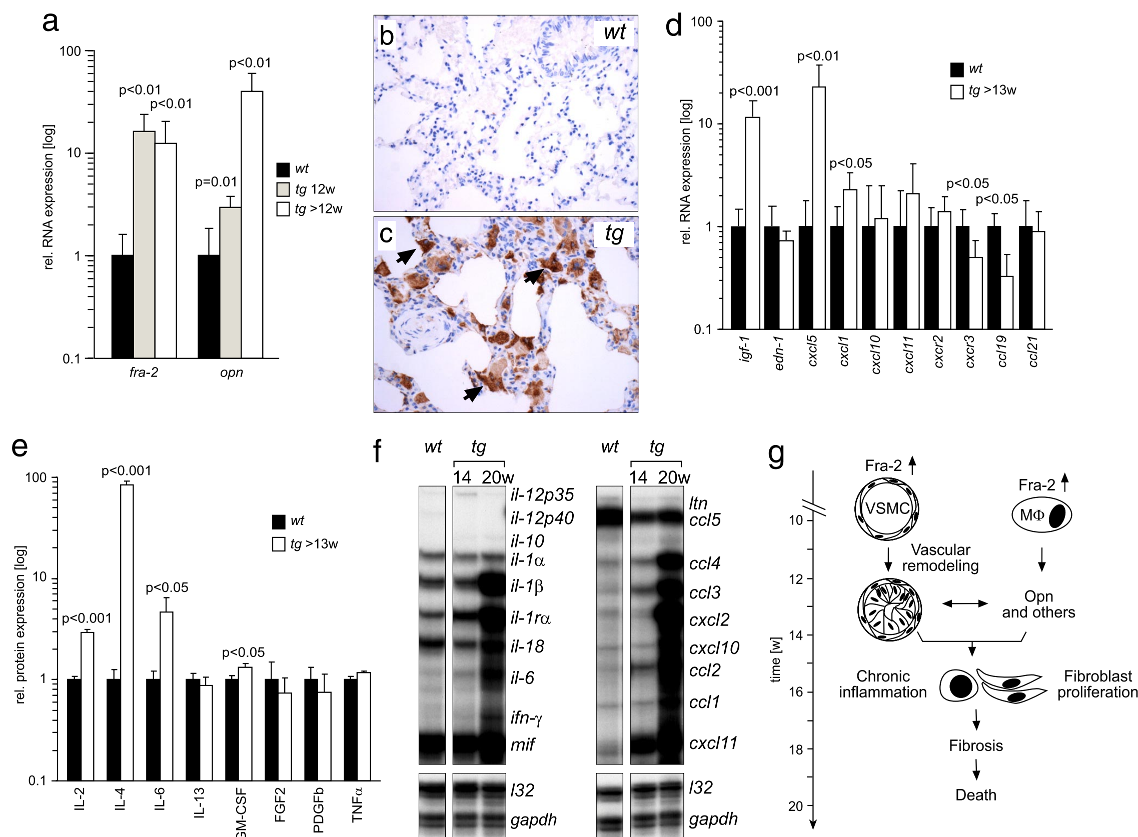

Fig. 4. Molecular factors involved in pulmonary fibrosis in *fra-2*^{tg} mice. (*a*) Expression of *fra-2* and osteopontin (*opn*) was analyzed by quantitative RT-PCR at the indicated time points ($n \geq 5$). (*b* and *c*) Immunohistochemistry reveals that osteopontin, absent from the wild type (*b*), was predominantly expressed by alveolar macrophages (*c*, arrows) in *fra-2*^{tg} lungs (17 weeks of age, $n = 3$). (*d*) Expression of fibrosis-related factors in *fra-2*^{tg} lungs was analyzed by quantitative RT-PCR ($n \geq 5$). *igf-1*, insulin like growth factor 1; *edn-1*, endothelin 1. (*e*) ELISA demonstrating increased cytokine protein expression of IL-2, IL-4, IL-6, and GM-CSF in lungs of *fra-2*^{tg} mice ($n \geq 4$). (*f*) Pulmonary expression of cytokines/chemokines in *fra-2*^{tg} (*tg*) mice that appeared healthy (14 weeks) or obviously sick (20 weeks). *l32* and *gapdh* were used as loading controls. (*g*) Proposed pathway leading to pulmonary fibrosis in *fra-2*^{tg} mice. Increased activity of Fra-2 in VSMCs, pulmonary epithelium (not shown), and alveolar macrophages (MΦ) induces aberrant vascular remodeling at ≈12 weeks of age, presumably by regulating osteopontin expression. These alterations lead to chronic inflammation, tissue damage, expression of profibrogenic factors such as IL-4, subsequent activation and proliferation of matrix-producing cells, fibrosis, and premature mortality.

evaluated by Fra-2 immunohistochemistry on patient samples of pulmonary fibrosis. Fra-2 was weakly expressed in some bronchial epithelial cells and occasionally in VSMCs of pulmonary arteries in control samples ($n = 5$) (Fig. 5*a* and Table S2). In contrast, consistently strong nuclear expression of Fra-2 was detectable in human samples of IPF with the histopathological picture of usual interstitial pneumonia ($n = 20$). Similar immunoreactivity was observed in immune-mediated cases of pulmonary fibrosis with the pathological picture of NSIP ($n = 7$) and cases of systemic sclerosis presenting as NSIP ($n = 7$) (Fig. 5 *b*–*d* and Table S2). In these samples, strong Fra-2 expression was detected in most bronchial and pneumocytic epithelial cells, fibroblastic foci, endothelial cells, and VSMCs of pulmonary arteries (Fig. 5). Moreover, expression of Fra-2 was observed in alveolar macrophages but not in infiltrating lymphocytes (data not shown). Increased expression of Fra-2 in human samples was also quantified by histomorphometry (Fig. 5*e*). These data suggest that increased Fra-2 expression may be an important profibrogenic event in various types of human pulmonary fibrosis.

Discussion

Genetically modified mice have provided important insights into the contribution of several Fos/AP-1 proteins to inflammation, bone biology, and cancer (1, 21, 22). The biological functions of the Fos-related protein Fra-2 are less well defined. Fra-2-deficient pups die postnatally for as-yet-unknown reasons (5). In this study, we have generated a transgenic mouse model for Fra-2 that revealed an unexpected profibrogenic function of this Fos protein in a variety of tissues but most prominently in the lung. Interestingly, a similar phenotype has not been observed previously in CMV-*fra-2*-transgenic mice (23) in which transgene expression was not detectable in the lung and low in other organs.

The manifestation of fibrosis in *fra-2*^{tg} mice resembles human systemic sclerosis, an autoimmune disease with generalized fibrosis that frequently affects the lung. However, sera of *fra-2*^{tg} mice were negative for autoantibodies directed against endothelial cells, topoisomerase I, and other antigens frequently associated with systemic sclerosis (data not shown). Moreover, disease was not altered in the absence of functional B and T lymphocytes, which argues against an autoimmune disease etiology in *fra-2*^{tg} mice.

Importantly, *fra-2*^{tg} mice represent a model for IPF or NSIP and could be used to further unravel the unknown pathomechanisms of these fatal lung diseases. Neointima formation and obliteration of pulmonary arteries were the first apparent alterations in *fra-2*^{tg} lungs. Intriguingly, intimal proliferation and medial thickening of muscular pulmonary arteries and pulmonary veins is frequently observed in patients with IPF (14) and pulmonary fibrosis associated with systemic sclerosis (24) and

Fig. 5. Fra-2 is strongly expressed in human pulmonary fibrosis as determined by immunohistochemistry. (*a*) In control samples, most nuclei were negative for Fra-2 (blue-stained nuclei). Nuclear localization of Fra-2 (brown-stained nuclei) was detected in some bronchial epithelial cells (black arrowheads, right magnification), whereas almost no expression was observed in VSMCs (red arrowheads, left magnification). (*b* and *c*) Strong nuclear localization of Fra-2 in two representative samples from patients diagnosed as IPF (a comparable signal for Fra-2 was observed in all IPF samples). Expression of Fra-2 was strongest in bronchial and pneumocytic epithelia (black arrowheads, right magnification in *b*), fibroblastic foci (short arrows in *b* and *c*, magnification in *c*), endothelial cells and VSMCs of pulmonary arteries (red arrowheads and left magnification in *b*). (*d*) Fra-2 expression in lung samples of immunologically determined systemic sclerosis (SSc). Note the vascular remodeling of pulmonary arteries with prominent Fra-2 staining in VSMCs (red arrowheads, magnification). (Scale bars: 100 μm.) (*e*) Tissue cytometric analysis in control, IPF, and systemic sclerosis samples confirmed up-regulation of Fra-2 expression. Representative examples are shown. Fra-2-negative nuclei and Fra-2-positive nuclei were counted, and the signal intensity was quantified by using HistoQuest software (TissueGnostics). Four randomly chosen fields on control, IPF, and systemic sclerosis sections were quantified and are shown as merged images.

may cause pulmonary arterial hypertension. It is widely believed that these alterations and pulmonary hypertension are secondary events without major impact on the course of fibrosis. However, a recent report has positively correlated pulmonary arterial changes with fibrosis in IPF (12). This report and other findings have raised the question whether the pathogenesis of pulmonary fibrosis and pulmonary hypertension may possibly be linked (11, 25). In humans, pulmonary arterial hypertension does not necessarily cause pulmonary fibrosis (25), but additional factors could indeed link vascular disease and fibrosis. In the light of these findings, it is tempting to speculate that increased expression of Fra-2 in various pulmonary cell types creates a microenvironment that leads to vascular disease and subsequent fibrosis.

Fra-2 can mediate obliteration of pulmonary arteries by two different mechanisms. AP-1 is activated by various proliferative signals such as PDGF in pulmonary arterial smooth muscle cells (SMCs) *in vitro* (26) and mediates VSMC proliferation in injured carotid arteries *in vivo* (27). The hyperproliferation of pulmonary arterial SMCs observed in *fra-2*^{tg} mice could thus occur in a cell-autonomous manner due to transgene expression. On the other hand, proliferation of VSMCs could be induced by soluble and Fra-2-dependent factors. Interestingly, expression of osteopontin coincided with the onset of vascular remodeling at 12 weeks of age and was the earliest factor up-regulated in *fra-2*^{tg} mice. Osteopontin has been implicated in the pathogenesis of various lung diseases in humans (19) and likely contributes substantially to the vascular alterations and fibrosis observed in *fra-2*^{tg} lungs. This possibility is substantiated by previous findings that osteopontin-transgenic mice show neointimal proliferation upon challenging the aorta (28) and that osteopontin-null mice develop reduced lung fibrosis after bleomycin instillation (29). Interestingly, several reports have shown that osteopontin expression is directly regulated by AP-1 in VSMCs and macrophages (17, 18, 20), and Fra-2 may be part of this regulatory AP-1 complex. Thus, induction of osteopontin expression in alveolar macrophages and pulmonary epithelium by Fra-2 could be an important molecular event that triggers vascular alterations, attracts inflammatory cells, and leads to fibrosis in *fra-2*^{tg} mice. However, Fra-2-dependent osteopontin expression in inflammatory cells is likely not sufficient to cause fibrosis, suggesting that an additional stimulus or Fra-2 expression in other cell types is required to trigger the onset of disease.

Vascular remodeling in *fra-2*^{tg} lungs was frequently associated with inflammation and expression of several growth factors and chemokines/cytokines involved in the pathogenesis of human pulmonary fibrosis and bleomycin-induced pulmonary fibrosis in mice such as IGF-1, CXCL5, IL-4, IL-1β, CCL2, and CCL3 (16, 30–32). These factors likely contribute to the progression of pulmonary fibrosis, e.g., by regulating collagen production by fibroblasts (33), and may at least in part be controlled by Fra-2/AP-1. Interestingly, the expression of TGFβ members was not elevated during early stages of disease development in *fra-2*^{tg} mice, although it has been shown that AP-1 activates the TGFβ_1 promoter in macrophages upon IL-13 stimulation, thereby promoting bleomycin-induced pulmonary fibrosis (34). Our findings suggest that this profibrogenic mechanism is not essential in *fra-2*^{tg} mice.

In summary, our findings reveal a profibrogenic function of the transcription factor Fra-2 and that *fra-2*^{tg} mice may serve as a promising animal model for devastating fibroproliferative diseases such as pulmonary fibrosis. Moreover, we propose that Fra-2-mediated osteopontin expression contributes to vascular remodeling, chronic inflammation, and subsequent fibrosis observed in the lung of transgenic mice and possibly in human patients.

Materials and Methods

Generation of *fra-2*^{tg} Mice. The full-length mouse *fra-2* was isolated from a λ library and cloned into the H2-c-*fos*LTR vector as described (2). An IRES-GFP-LTR sequence was cloned 3′ of *fra-2*. Transgenic mice were kept on a mixed genetic background (C57BL/6 $\times$ CBA) and nontransgenic littermates were used as controls. Pulmonary fibrosis and premature mortality were not altered by backcrossing to C57BL/6 or 129/Sv for more than six generations.

Southern and Western Blotting and ELISA. Genomic DNA was digested with HindIII, yielding a 12-kb fragment for the wild-type *fra-2* allele and a 10.5-kb fragment for the transgenic *fra-2* allele. A 0.6-kb KpnI fragment from exon 2 of *fra-2* was used as a probe. Western blotting was performed by using antibodies against Fra-2 or Actin (Sigma). ELISA of lung lysates was performed by using Bioplex mouse cytokine arrays (Bio-Rad).

RNase-Protection Assay. The RNase-protection assay was performed by using the RiboQuant multiprobe RNase protection assay systems mFos/Jun, mAPO1,

mAPO2, mAPO3, mCK5c, mCK2b, and mCK3b (PharMingen) according to the manufacturer's protocol.

PCR Analysis. PCR for genotyping of *fra-2*^{tg} mice was performed with primers h2-fos-up: agtctggcctgcgggtctct and rep19: ccacaacttacagcggtgaagtat detecting the transgene (560 bp). For RT-PCR, light cycler Fast Start DNA Master SYBR Green (Roche Diagnostics) was used. Primer sequences are available upon request. RNA from at least three animals was analyzed in duplicate, and the expression levels of transcripts were calculated with the comparative CT (threshold concentration) method. The individual RNA levels were normalized for tubulin or *hprt* and are depicted as relative expression levels.

Histology, Immunohistochemistry, and Tissue Cytometry. Tissues were fixed in neutral-buffered 4% paraformaldehyde, and sections were stained with H&E or Chromotrop Anilinblue (CAB) by using standard procedures. Immunohistochemistry was performed by using antibodies against Ki67 (Novocastra), αSMA (Sigma), and osteopontin (R&D). Staining of human samples was performed with anti-Fra-2 antibodies (Santa Cruz Biotechnology H103 and L15). Transgene expression was assessed by direct fluorescence of transgene-encoded IRES-GFP on cryosections.

Fra-2 expression in human samples was judged and quantified independently by two experienced pathologists (L.K. and H.P.). The staining intensity was quantified by tissue cytometry using the HistoQuest analysis software (TissueGnostics). HistoQuest separates the antibody-mediated chromogen stain and the counterstain. Results are displayed in dot plots, with each dot representing a single cell in the tissue sample.

Bone Marrow Reconstitution Experiments. Reconstitution experiments were performed with littermates as donors and recipients (mixed C57BL/6 × 129/Sv background). Bone marrow cells (4×10^6 cells) were injected into the tail vein of lethally irradiated (9.5 Gy) female recipient mice (6–10 weeks old). Control mice were injected with PBS and died a few days after irradiation. Reconstituted mice were killed at the time points indicated in Table S1.

Statistical Analysis. Data in bar graphs represent mean ± SD. The nonparametric Mann–Whitney test and nondirectional unpaired Student's *t* test were used for statistical analysis as appropriate.

More information is available in the *SI Materials and Methods*.

ACKNOWLEDGMENTS. We thank Drs. J. Smolen and J. Varga and members of the Wagner laboratory for critical reading of the manuscript and helpful discussions; H. C. Theussl for egg injections; Drs. C. Mayerl, G. Steiner, and G. Wick for serum analysis of autoantibodies; M. Schlederer for histomorphometrical quantification; and M. Yaniv for providing antibody. This work was supported in part by Austrian Science Fund Grant SFB-F28 and a Deutsche Forschungsgemeinschaft postdoctoral fellowship (to P.H.). The Research Institute of Molecular Pathology is funded by Boehringer Ingelheim and supported by the Austrian Industrial Research Promotion Fund. R.E. and R.Z. are funded by the Ludwig Boltzmann Society. E.F.W. is supported by the Cells into Organs Network of Excellence and is a participant in the Sixth European Union Framework Program.

1. Eferl R, Wagner EF (2003) AP-1: A double-edged sword in tumorigenesis. *Nat Rev Cancer* 3:859–868.
2. Grigoriadis AE, Schellander K, Wang ZQ, Wagner EF (1993) Osteoblasts are target cells for transformation in c-fos transgenic mice. *J Cell Biol* 122:685–701.
3. Jochum W, *et al.* (2000) Increased bone formation and osteosclerosis in mice overexpressing the transcription factor Fra-1. *Nat Med* 6:980–984.
4. Sabatakos G, *et al.* (2000) Overexpression of DeltaFosB transcription factor(s) increases bone formation and inhibits adipogenesis. *Nat Med* 6:985–990.
5. Eferl R, Zenz R, Theussl HC, Wagner EF (2007) Simultaneous generation of fra-2 conditional and fra-2 knock-out mice. *Genesis* 45:447–451.
6. Nicholson AG, Colby TV, Wells AU (2002) Histopathological approach to patterns of interstitial pneumonia in patient with connective tissue disorders. *Sarcoidosis Vasc Diffuse Lung Dis* 19:10–17.
7. Selman M, King TE, Pardo A (2001) Idiopathic pulmonary fibrosis: Prevailing and evolving hypotheses about its pathogenesis and implications for therapy. *Ann Intern Med* 134:136–151.
8. Hinz B, *et al.* (2007) The myofibroblast: One function, multiple origins. *Am J Pathol* 170:1807–1816.
9. Phillips RJ, *et al.* (2004) Circulating fibrocytes traffic to the lungs in response to CXCL12 and mediate fibrosis. *J Clin Invest* 114:438–446.
10. Hamada K, *et al.* (2007) Significance of pulmonary arterial pressure and diffusion capacity of the lung as prognosticator in patients with idiopathic pulmonary fibrosis. *Chest* 131:650–656.
11. Nathan SD, Noble PW, Tuder RM (2007) Idiopathic pulmonary fibrosis and pulmonary hypertension: Connecting the dots. *Am J Respir Crit Care Med* 175:875–880.
12. Parra ER, *et al.* (2005) Heterogeneous remodeling of lung vessels in idiopathic pulmonary fibrosis. *Lung* 183:291–300.
13. Lee CG, *et al.* (2004) Early growth response gene 1-mediated apoptosis is essential for transforming growth factor beta1-induced pulmonary fibrosis. *J Exp Med* 200:377–389.
14. Katzenstein AL, Myers JL (1998) Idiopathic pulmonary fibrosis: Clinical relevance of pathologic classification. *Am J Respir Crit Care Med* 157:1301–1315.
15. Kim KK, *et al.* (2006) Alveolar epithelial cell mesenchymal transition develops *in vivo* during pulmonary fibrosis and is regulated by the extracellular matrix. *Proc Natl Acad Sci USA* 103:13180–13185.
16. Agostini C, Gurrieri C (2006) Chemokine/cytokine cocktail in idiopathic pulmonary fibrosis. *Proc Am Thorac Soc* 3:357–363.
17. Bidder M, *et al.* (2002) Osteopontin transcription in aortic vascular smooth muscle cells is controlled by glucose-regulated upstream stimulatory factor and activator protein-1 activities. *J Biol Chem* 277:44485–44496.
18. Ogawa D, *et al.* (2005) Liver X receptor agonists inhibit cytokine-induced osteopontin expression in macrophages through interference with activator protein-1 signaling pathways. *Circ Res* 96:e59–67.
19. Pardo A, *et al.* (2005) Up-regulation and profibrotic role of osteopontin in human idiopathic pulmonary fibrosis. *PLoS Med* 2:e251.
20. Renault MA, *et al.* (2003) AP-1 is involved in UTP-induced osteopontin expression in arterial smooth muscle cells. *Circ Res* 93:674–681.
21. Jochum W, Passegue E, Wagner EF (2001) AP-1 in mouse development and tumorigenesis. *Oncogene* 20:2401–2412.
22. Wagner EF, Eferl R (2005) Fos/AP-1 proteins in bone and the immune system. *Immunol Rev* 208:126–140.
23. McHenry JZ, Leon A, Matthaei KI, Cohen DR (1998) Overexpression of fra-2 in transgenic mice perturbs normal eye development. *Oncogene* 17:1131–1140.
24. Varga J, Abraham D (2007) Systemic sclerosis: A prototypic multisystem fibrotic disorder. *J Clin Invest* 117:557–567.
25. Hunninghake GW, Schwarz MI (2007) State of the art. Does current knowledge explain the pathogenesis of idiopathic pulmonary fibrosis?: A perspective. *Proc Am Thorac Soc* 4:449–452.
26. Rothman A, Wolner B, Button D, Taylor P (1994) Immediate-early gene expression in response to hypertrophic and proliferative stimuli in pulmonary arterial smooth muscle cells. *J Biol Chem* 269:6399–6404.
27. Ahn JD, *et al.* (2002) Inhibitory effects of novel AP-1 decoy oligodeoxynucleotides on vascular smooth muscle cell proliferation in vitro and neointimal formation in vivo. *Circ Res* 90:1325–1332.
28. Isoda K, *et al.* (2002) Osteopontin plays an important role in the development of medial thickening and neointimal formation. *Circ Res* 91:77–82.
29. Berman JS, *et al.* (2004) Altered bleomycin-induced lung fibrosis in osteopontin-deficient mice. *Am J Physiol* 286:L1311–L1318.
30. Huaux F, Liu T, McGarry B, Ullenbruch M, Phan SH (2003) Dual roles of IL-4 in lung injury and fibrosis. *J Immunol* 170:2083–2092.
31. Strieter RM, Gomperts BN, Keane MP (2007) The role of CXC chemokines in pulmonary fibrosis. *J Clin Invest* 117:549–556.
32. Uh ST, *et al.* (1998) Morphometric analysis of insulin-like growth factor-I localization in lung tissues of patients with idiopathic pulmonary fibrosis. *Am J Respir Crit Care Med* 158:1626–1635.
33. Gharaee-Kermani M, Nozaki Y, Hatano K, Phan SH (2001) Lung interleukin-4 gene expression in a murine model of bleomycin-induced pulmonary fibrosis. *Cytokine* 15:138–147.
34. Fichtner-Feigl S, Strober W, Kawakami K, Puri RK, Kitani A (2006) IL-13 signaling through the IL-13alpha2 receptor is involved in induction of TGF-beta1 production and fibrosis. *Nat Med* 12:99–106.